Two-component soliton model for proton transport in hydrogen-bonded molecular chains

Jesper Halding and Peter S. Lomdahl
Theoretical Division and Center for Nonlinear Studies, Los Alamos National Laboratory, Los Alamos, New Mexico 87545
(Received 16 October 1987)

We propose a two-component soliton model for proton storage and transport in hydrogen-bonded quasi-one-dimensional chains. The model is investigated both analytically and by molecular-dynamics simulations. At 310 K we find that in certain regions of the parameter space it is possible, from realistic initial conditions, to excite a kink in the proton sublattice. For certain parameter values and initial conditions the kink is excited just to be annihilated shortly after. For other parameter values the kink continues to travel for much longer times. Therefore the presented model can explain the essential physics of proton storage as well as proton transport in hydrogen-bonded substances.

I. INTRODUCTION

The transport of electrical charge in molecular and biological systems has been studied extensively during the last decades.[1-12] The reason is that it is essential to understand simple transport phenomena in such systems at the molecular level in order to gain insight in more complicated life processes. The proton conductivity in hydrogen-bonded molecules is remarkably high and in fact certain of these materials have been called protonic semiconductors.[1] A theory for proton transport in quasi-one-dimensional hydrogen-bonded chains has applications in several biological systems: (i) α-helix proteins traversing biological membranes, connecting the intracellular and the extracellular regions, thereby providing a channel for proton transport through the membrane, (ii) several solid-state systems showing very high proton conductivity (see Refs. 3 and 10), (iii) icelike structures showing a proton mobility only an order of magnitude less than in metals.[3,4] In Ref. 1 it was suggested that there is an analogy between the motion of protons in a hydrogen-bonded molecular chain and the motion of dislocations in crystals. The hydrogen bonded system

$$\cdots A\text{—H}\cdots A\text{—H}\cdots A\text{—H}\cdots A\text{—H}\cdots A\text{—H}\cdots,$$

where the dotted-line segments indicate the hydrogen bonds, and the A's symbolize some (heavy) ions with negative charge, was modeled by assuming that the protons were connected by springs and moving between each pair of fixed heavy ions in a symmetrical double-well potential. In the case of an external applied electrical field, it was found that the barrier height for cooperative proton motion was much smaller than the barrier for individual proton motion, and it was thereby concluded that the model qualitatively could explain the high mobility of protons in hydrogen-bonded substances. Due to this effective transport of protons it is not surprising that the concept of soliton theory has been introduced in such systems.[4-6,9-12] In Ref. 4 another model for a slightly different molecular geometry was proposed. The protons were again moving in a double-well potential, but now also the heavy ions were allowed to move. The idea was that a reduction of the distance between two neighbor heavy ions induced a reduction of the barrier height in the potential experienced by the proton between these surrounding molecules (see Fig. 1). It turned out that insertion of a traveling-wave assumption in the continuum version of the derived equations leads to exact soliton solutions in the proton sublattice as well as in the heavy ion sublattice at a particular speed of the traveling wave. So a transition region between protons being in the left well, and protons being in the right well (kink) could travel along the chain together with a compression in the heavy ion sublattice without any loss of energy. Other papers have addressed the same model from numerical and analytical points of view taking into account additional features, e.g., effects of an applied external electrical field and damping,[11,12] stability of the solitons was investigated in Refs. 9 and 10. In Sec. II we describe what the potential in which the protons move looks like, and how it is altered when the distance between the two surrounding heavy ions changes. Then in Sec. III we present the model Hamiltonian and derive the corresponding dynamical equations. In Sec. IV we study the continuum limit of the derived equations and show that there exists soliton solutions. Section V contains the details of our molecular-dynamics calculations, and explains how we incorporate temperature effects. Finally we conclude the paper in Sec. VI.

II. THE HYDROGEN-BOND POTENTIAL

In this paper we report on molecular dynamics (MD) calculations in a thermalized one-dimensional molecular

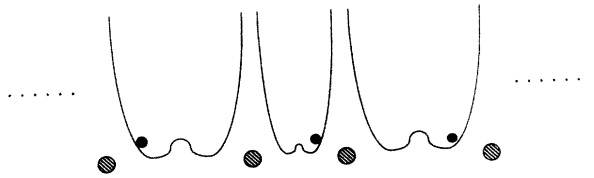

FIG. 1. Schematic picture of the hydrogen-bonded molecular chain and the effective potential for the proton.

lattice, consisting of N heavy ions and $N-1$ protons. The lattice constant is denoted l, and between each pair of heavy ions, a proton is moving in a double-well potential, modeled as

$$V(u_n)=\varepsilon_0(1-u_n^2/u_0^2)^2 . \tag{1}$$

Here u_n denotes the displacement of the nth proton relative to the midpoint between the two surrounding heavy ions, ε_0 is the barrier height, and u_0 is the distance along the chain from the top of the barrier to one of the minima in the double-well potential when the distance between the two heavy ions is the equilibrium distance (see Fig. 2). From Ref. 1 we obtain $\varepsilon_0=0.22$ eV, $u_0=0.39\times10^{-10}$ m, and $l=2.76\times10^{-10}$ m. Here we will use the same fundamental mechanism for proton transport in hydrogen-bonded systems as in Refs. 4 and 9–12, namely, that both the barrier height and the distance from the top of the barrier to one of the minima in the potential change when the relative distance ρ_n between the two surrounding heavy ions changes. So we write what we call the effective potential in the following way:

$$V^{\text{eff}}(u_n,\rho_n)=a(\rho_n)u_n^4+b(\rho_n)u_n^2+c(\rho_n) , \tag{2}$$

where

$$\rho_n=x_{n+1}-x_n \tag{3}$$

and

$$V^{\text{eff}}(u_n,0)=V(u_n) . \tag{4}$$

In (3) x_n is the absolute position of the nth heavy ion, so $\rho_n>0$ is an elongation of the distance between the heavy ions surrounding the nth proton, and $\rho_n<0$ is a compression. The unknown functions a, b, and c will be determined according to experimental data in the following. The barrier height $\varepsilon(\rho_n)$ and the distance along the chain from the top of the barrier to one of the minima $u(\rho_n)$ is easily calculated from (2). We obtain

$$u(\rho_n)=\left[\frac{-b(\rho_n)}{2a(\rho_n)}\right]^{1/2} , \tag{5}$$

$$\varepsilon(\rho_n)=\frac{1}{4}\frac{b(\rho_n)^2}{a(\rho_n)} . \tag{6}$$

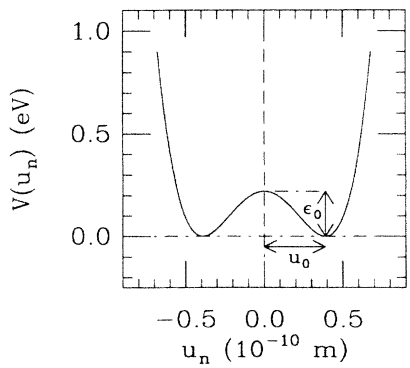

FIG. 2. Double-well potential corresponding to equilibrium position of the two surrounding heavy ions.

Experimental results,[13,14] show that $\varepsilon(\rho_n)$ can be assumed to be second order in ρ_n and that $u(\rho_n)$ can be modeled by a square-root expression in ρ_n. The simplest way to achieve this is by adopting the following expressions for a and b:

$$a(\rho_n)=k_1 , \tag{7}$$

$$b(\rho_n)=k_2(\rho_n+k_3) , \tag{8}$$

k_1, k_2, and k_3 being constants. There is evidence that the double-well potential collapses to a single-well potential for short hydrogen bonds,[14] so we put $k_3=0.1\times l=0.276\times10^{-10}$ m, meaning that the double-well potential degenerates to a single-well potential at 10% compression of the lattice spacing. Inserting (7) and (8) in (5) and (6), and making use of $u(\rho_n=0)=u_0$ and $\varepsilon(\rho_n=0)=\varepsilon_0$, we obtain

$$k_1=\frac{\varepsilon_0}{u_0^4} , \tag{9}$$

$$k_2=-\frac{2\varepsilon_0}{u_0^2k_3} . \tag{10}$$

Figure 3 shows ε and u as functions of ρ_n as calculated from (5) and (6). Since, obviously, $c(\rho_n)=\varepsilon(\rho_n)$ the effective potential (2) is now known as a function of the constants ε_0, u_0, and k_3, and in Fig. 4, we show how the double well looks in the equilibrium position (as in Fig. 2) for 5% elongation of the distance between the surrounding heavy ions and for 5% compression of this distance.

III. THE MODEL HAMILTONIAN

The Hamiltonian describing the system consists of three parts: the proton part, the heavy ion part, and a part taking into account that the double-well potential changes with ρ_n. Since we want to have free boundaries, the proton part of the total Hamiltonian is

$$H_p=\sum_{n=1}^{N-1}{}' \tfrac{1}{2}m(\dot{u}_n)^2+V(u_n)+\tfrac{1}{2}m\omega_1^2(u_{n+1}-u_n)^2 , \tag{11}$$

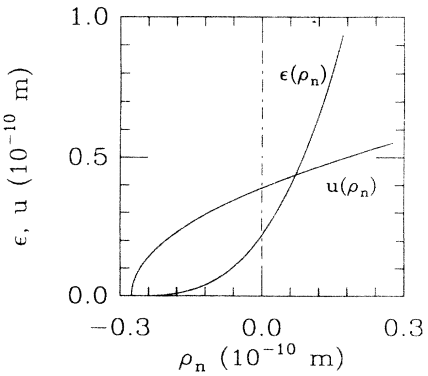

FIG. 3. The barrier height ε and the distance along the chain from the top of the barrier to one of the minima u as a function of the relative distance ρ_n between the two surrounding heavy ions.

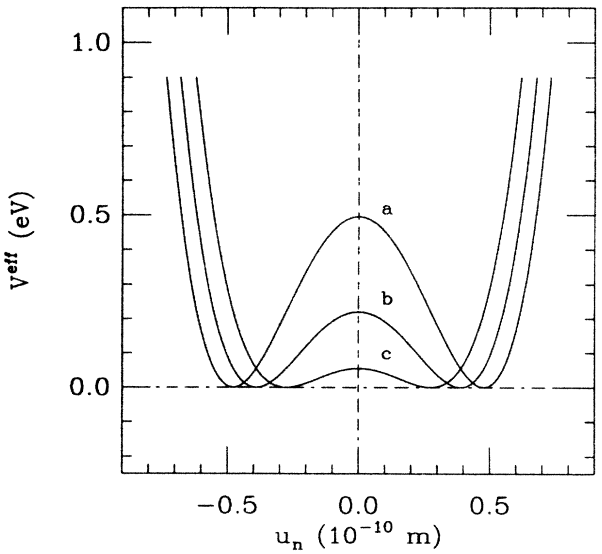

FIG. 4. Effective potential as a function of u_n; *a*, 5% elongation of distance between surrounding heavy ions; *b*, equilibrium distance (corresponds to Fig. 2); *c*, 5% compression of the distance between surrounding heavy ions.

and the heavy ion contribution to the total Hamiltonian is

$$H_0=\sum_{n=1}^{N}{}' \tfrac{1}{2}M(\dot{x}_n)^2+\tfrac{1}{2}M\Omega_1^2(x_{n+1}-x_n)^2 . \tag{12}$$

In (11) m is the mass of the proton and the last term describes the normal dispersive coupling with characteristic frequency ω_1 between neighboring protons. This is similar to (12), where M is the mass of each of the heavy ions. The primes on the summation signs in (11) and (12) indicates that the last terms only are summed to $N-2$ and $N-1$, respectively. Finally the interaction Hamiltonian is obtained by subtracting $V(u_n)$ from the effective potential $V^{\text{eff}}(u_n,\rho_n)$ [we have already counted it in (11)]. This means that the effect of changing barrier height for a proton when changing the distance between the two surrounding heavy ions is taken into account through the interaction Hamiltonian. With the definitions

$$\chi_1=-k_2=\frac{2\varepsilon_0}{u_0^2k_3}>0 , \tag{13}$$

$$\chi_2=\frac{u_0^2}{2k_3}>0 , \tag{14}$$

$$\chi_3=2k_3>0 , \tag{15}$$

we have the following expression for the interaction Hamiltonian:

$$H_i=-\chi_1\sum_{n=1}^{N-1}\rho_n[u_n^2-\chi_2(\rho_n+\chi_3)] . \tag{16}$$

From the total Hamiltonian we can derive the following dynamical equations:

$$\ddot{u}_n=\omega_1^2(u_{n+1}-2u_n+u_{n-1})+\frac{4\varepsilon_0}{mu_0^2}u_n\left[1-\frac{u_n^2}{u_0^2}\right]+\frac{2\chi_1}{m}u_n(x_{n+1}-x_n),\quad 1<n<N-1 \tag{17}$$

$$\ddot{x}_n=\left[\Omega_1^2+\frac{2\chi_1\chi_2}{M}\right](x_{n+1}-2x_n+x_{n-1})-\frac{\chi_1}{M}(u_n^2-u_{n-1}^2),\quad 1<n<N . \tag{18}$$

At the boundaries we have

$$\ddot{u}_1=\omega_1^2(u_2-u_1)+\frac{4\varepsilon_0}{mu_0^2}u_1\left[1-\frac{u_1^2}{u_0^2}\right]+\frac{2\chi_1}{m}u_1(x_2-x_1) , \tag{19}$$

$$\ddot{u}_{N-1}=\omega_1^2(-u_{N-1}+u_{N-2})+\frac{4\varepsilon_0}{mu_0^2}u_{N-1}\left[1-\frac{u_{N-1}^2}{u_0^2}\right]+\frac{2\chi_1}{m}u_{N-1}(x_N-x_{N-1}) , \tag{20}$$

$$\ddot{x}_1=\left[\Omega_1^2+\frac{2\chi_1\chi_2}{M}\right](x_2-x_1)-\frac{\chi_1}{M}u_1^2+\frac{\chi_1\chi_2\chi_3}{M} , \tag{21}$$

$$\ddot{x}_N=\left[\Omega_1^2+\frac{2\chi_1\chi_2}{M}\right](x_{N-1}-x_N)+\frac{\chi_1}{M}u_{N-1}^2-\frac{\chi_1\chi_2\chi_3}{M} . \tag{22}$$

The system (17)–(22) constitutes the dynamical equations we will integrate in Sec. IV.

IV. THE CONTINUUM LIMIT

Before we proceed to a numerical investigation of the system (17)–(22), it is interesting to look at the two coupled nonlinear partial differential equations, appearing in the continuum limit and for small displacements. We obtain

$$u_{tt}-\omega_1^2l^2u_{yy}-\frac{4\varepsilon_0}{mu_0^2}u\left[1-\frac{u^2}{u_0^2}\right]-\frac{2\chi_1}{m}ulx_y=0 , \tag{23}$$

$$x_{tt}-\left[\Omega_1^2+\frac{2\chi_1\chi_2}{M}\right]l^2x_{yy}+2\frac{\chi_1}{M}luu_y=0 , \tag{24}$$

where y denotes the continuous longitudinal space variable. Introducing the sound speed in the proton sublattice, c_1, and in the heavy ion sublattice, c_2, as

$$c_1^2=l^2\omega_1^2 \tag{25}$$

and

$$c_2^2=\left[\Omega_1^2+\frac{2\chi_1\chi_2}{M}\right]l^2 , \tag{26}$$

and introducing a moving frame, $\xi=(y-vt)/l$, v being the velocity of this frame, we arrive at

$$\frac{1}{l^2}(c_1^2-v^2)u_{\xi\xi}+\frac{4\varepsilon_0}{mu_0^2}u\left[1-\frac{u^2}{u_0^2}\right]+\frac{2\chi_1}{m}ux_\xi=0\ , \tag{27}$$

$$\frac{1}{l^2}(v^2-c_2^2)x_{\xi\xi}+2\frac{\chi_1}{M}uu_\xi=0\ . \tag{28}$$

From (28) we get (for $v^2\neq c_2^2$)

$$\frac{d}{d\xi}\left[\frac{1}{l^2}(v^2-c_2^2)x_\xi+\frac{\chi_1}{M}u^2\right]=0 \tag{29}$$

or

$$x_\xi=\frac{l^2}{v^2-c_2^2}\left[-\frac{\chi_1}{M}u^2+\tilde{c}_1\right]\ , \tag{30}$$

where $\tilde{c}_1$ is an integration constant. This result can be substituted back in (27) yielding

$$\frac{1}{l^2}(c_1^2-v^2)u_{\xi\xi}+u^3\left[\frac{-4\varepsilon_0}{mu_0^4}-\frac{2\chi_1^2l^2}{mM(v^2-c_2^2)}\right]$$

$$+u\left[\frac{4\varepsilon_0}{mu_0^2}+\tilde{c}_1\frac{2\chi_1^2l^2}{m(v^2-c_2^2)}\right]=0\ . \tag{31}$$

This ϕ^4 equation has the well-known tanh kink solution.[4,11] Insertion of this solution in (30) then makes it possible to find x. We find (for $v^2\neq c_2^2$ and $v^2\neq c_1^2$)

$$u(\xi)=\pm u_0\tanh(A\xi) \tag{32}$$

and

$$x(\xi)=B\tanh(A\xi)\ , \tag{33}$$

where the constants A and B are given by the following expressions:

$$A=\left[\frac{2\varepsilon_0l^2}{(c_1^2-v^2)mu_0^2}+\frac{\chi_1^2l^4u_0^2}{mM(v^2-c_2^2)(c_1^2-v^2)}\right]^{1/2}\ , \tag{34}$$

$$B=\frac{l^2\chi_1u_0^2}{(v^2-c_2^2)MA}\ . \tag{35}$$

The antikink solution in the x variable means that the space derivative is an antisoliton, i.e., the kink in the proton sublattice travels along the chain together with a compression in the heavy ion sublattice. It is interesting that our continuum model supports soliton solutions for all velocities less than the sound velocities (c_1 and c_2), whereas the models in Refs. 4 and 9–12 only support such *analytical* solutions for one single value of this velocity.

V. MOLECULAR DYNAMICS DETAILS AND RESULTS

We include temperature effects by using a standard isokinetic MD method.[15,16] The equipartition theorem[17] states that both the heavy ion and the proton lattice have to be in thermal equilibrium, that is,

$$T=\left\langle\frac{M}{Nk_B}\left[\sum_{n=1}^{N}\dot{x}_n^2\right]\right\rangle \tag{36}$$

and

$$T=\left\langle\frac{m}{(N-1)k_B}\left[\sum_{n=1}^{N-1}\dot{u}_n^2\right]\right\rangle\ , \tag{37}$$

where $\langle\ \rangle$ indicates time average, T the temperature, and k_B Boltzmann's constant.

We use a standard fifth-order Runge-Kutta scheme to integrate the dynamical equations and rescale the molecular velocities, $\dot{x}_n$ and $\dot{u}_n$, at $t=i\Delta t$, $i=1,2,\ldots$, subject to the relations (36) and (37). This means that the rescaling factors for $\dot{x}_n$ and $\dot{u}_n$ become

$$\alpha_1^i=\left[\frac{NkT}{M\sum_{n=1}^{N}(\dot{x}_n^i)^2}\right]^{1/2} \tag{38}$$

and

$$\alpha_2^i=\left[\frac{(N-1)kT}{m\sum_{n=1}^{N-1}(\dot{u}_n^i)^2}\right]^{1/2}\ , \tag{39}$$

respectively.

The numerical calculations were performed in the following way. All the runs were with $N=100$ and $M=100\times m=1.67\times10^{-25}$ kg and in order to reduce the number of parameters we always took $\Omega=0.1\omega_1$. Our Runge-Kutta scheme runs with variable step size, but we read out the molecular velocities every $\Delta t=0.25\times10^{-14}$ sec to rescale by the factors (38) and (39). Variation of the tolerance parameter in the integrator and in Δt did not affect our results significantly. We subjected the dynamical equations (17)–(22) to random initial conditions (the positions of all protons randomly distributed around the left minima in the potentials), and integrated the system using the rescaling technique explained above until thermal equilibrium in both lattices was achieved. The relaxation time was always less than 10^{-13} sec. Then the system was excited by moving heavy ion no. 1 away from no. 2 until the distance between them was $1.1l$ (10% elongation). Simultaneously proton no. 1 was given a certain amount of kinetic energy in the direction towards proton no. 2. Then heavy ion no. 1 was released, and the system was allowed to move according to the dynamical equations including the scaling factors. We feel that this way of starting the system is more realistic than applying the continuum solution as initial conditions.

In Fig. 5 we show results from integrating the system (17)–(22) at 310 K from the initial conditions mentioned above. We define the kink location as the site no. closest to the zero crossing of u_n. In Fig. 5(a) we have $\omega_1=2.0\times10^{14}$ Hz, and $\Omega_1=2.0\times10^{13}$ Hz. When proton no. 1 is given the kinetic energy 2.0 eV, a kink is traveling about ten sites before it turns around and is annihilated after approximately 0.8 psec. If the input energy is increased to 3 eV, the kink is able to travel for a much longer time; in fact it is located around site no. 10 after

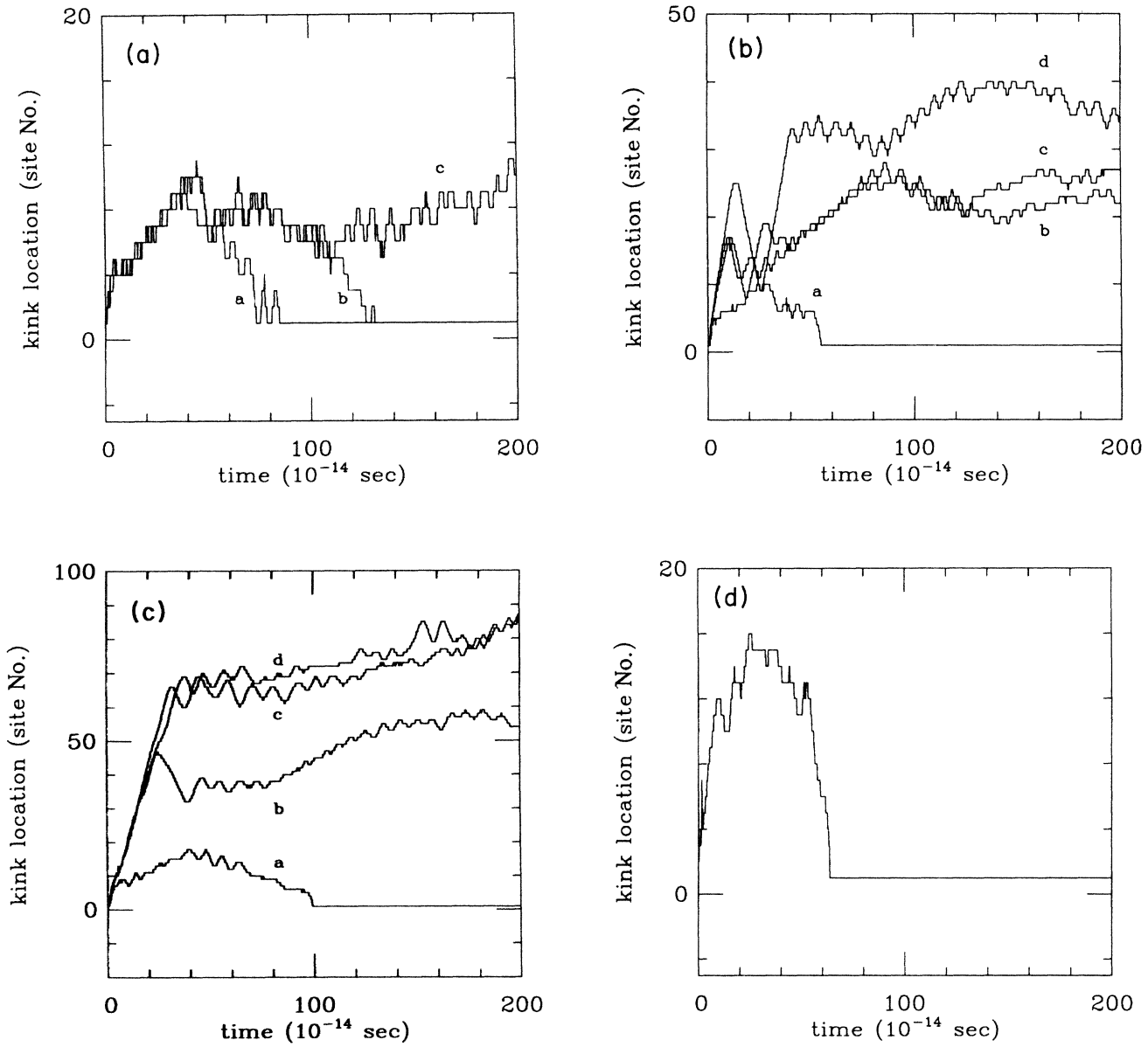

FIG. 5. Kink location as function of time after excitation for different values of ω_1 and kinetic energy input of proton no. 1. In all runs we have $\Omega_1=0.1\omega_1$. (a) $\omega_1=2\times10^{14}$ Hz. *a*, 2 eV, *b*, 4 eV, *c*, 3 eV. (b) $\omega_1=3\times10^{14}$ Hz. *a*, 3.5 eV, *b*, 4 eV, *c*, 6 eV, *d*, 5 eV. (c) $\omega_1=4\times10^{14}$ Hz. *a*, 5 eV, *b*, 6 eV, *c*, 7 eV, *d*, 8 eV. (d) $\omega_1=5\times10^{14}$ Hz. 8 eV.

2.0 psec. At an input energy of 4 eV the situation is in between. For values of the input energy above approximately 4.5 eV or below approximately 1.5 eV, it is not possible to even excite a kink, so there seems to be a "window" for the amount of kinetic input energy of proton no. 1 in which a kink can be excited and travel along the chain. In Fig. 5(b) we have increased the values of the basic frequencies of the system to $\omega_1=3.0\times10^{14}$ Hz and $\Omega_1=3.0\times10^{13}$ Hz. The same features as in Fig. 5(a) are observed, except that the input energy window now is located at higher values of this energy. Also, we see that the kinks are able to travel longer before they get pinned or turn around. In Fig. 5(c) we have $\omega_1=4.0\times10^{14}$ Hz and $\Omega_1=4.0\times10^{13}$ Hz, and now the kinks can travel even longer. For input energies between 7 and 8 eV we observe an interesting behavior. After excitation the kink moves about 70 sites along the chain without being affected significantly by the thermal noise. After having traveled this distance in about 0.3 psec, the kink velocity decreases to about 5% of its original value. Finally in Fig. 5(d), where we have $\omega_1=5.0\times10^{14}$ Hz and $\Omega_1=5.0\times10^{13}$ Hz, we find that the input energy window is very narrow, so we only show the result for 8 eV. Comparing the four pictures in Fig. 5, we see that there also is a window for the frequencies ω_1 and Ω_1 in which kink formation (and movement) is possible. Only in the interval 2×10^{14} Hz $<\omega_1<5\times10^{14}$ Hz (maintaining $\Omega_1=0.1\omega_1$) do we see kink excitation. It is interesting

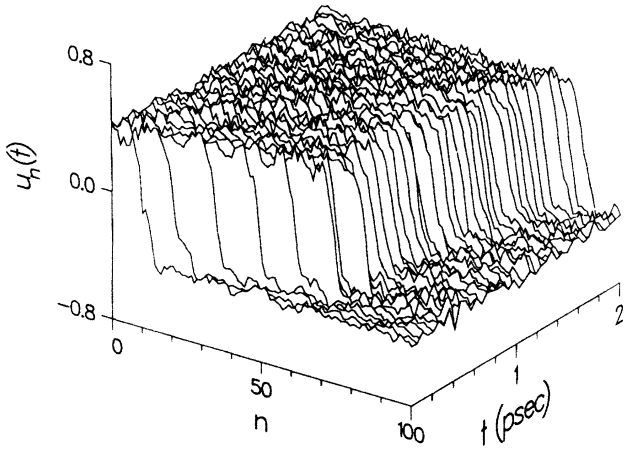

FIG. 6. Location of the protons as function of site no. n and time. Parameter values as in Fig. 5(c).

that the location of the interval for kink excitation compares favorably with what is known about these frequencies.[1,6] Finally, in Fig. 6 we show the location of the protons as function of the site no. and time. All parameter values are as described in Fig. 5(c). It is clearly seen that after getting excited, the kink moves with a high velocity out to approximately site no. 70. Thereafter its velocity decreases drastically.

VI. CONCLUDING REMARKS

We have proposed a new two-component one-dimensional molecular model for transport and storage of protons. We have not attempted to do a thorough parameter study, but have fixed some of these at what we believe are physical reasonable values. At realistic temperature and for realistic initial conditions, we find that there exist regions in the two-dimensional (proton kinetic energy input)-(ω_1) parameter space, where the model shows that kink formation and propagation is possible. In the cases where a kink starts moving and later turns around (before the end of the chain is reached) and is annihilated, the model describes storage of a proton: An excess proton can move into the chain at $t=0$ and be back at the same location at a later time. What makes the proton turn around in a real biological system could be, for example, changes in an electrical field experienced by the chain or changes in ion concentrations across a membrane. If the proton does not turn around before the end of the chain, the model describes proton transport in a hydrogen-bonded chain.

ACKNOWLEDGMENTS

The financial support of the Danish Research Council for Scientific and Industrial Research to one of the authors (J.H.) is acknowledged. This work was done under the auspices of the U.S. Department of Energy.

[1]J. H. Weiner and A. Askar, Nature **226**, 842 (1970).
[2]M. Eigen and L. De Maeyer, Proc. R. Soc. London, Ser. A **247**, 505 (1958).
[3]J. F. Nagle and M. Mille, J. Chem. Phys. **72**, 3959 (1980); also J. F. Nagle and H. J. Morowitz, Proc. Natl. Acad. Sci. U.S.A. **75**, 298 (1976).
[4]V. Ya. Antochencko, A. S. Davydov, and A. V. Zolotariuk, Phys. Status Solidi B **115**, 631 (1983).
[5]S. Yomosa, J. Phys. Soc. Jpn. **51**, 3318 (1982).
[6]S. Yomosa, J. Phys. Soc. Jpn. **52**, 1866 (1983).
[7]J. R. de la Vega, J. H. Busch, J. H. Schauble, K. L. Kunze, and B. E. Haggert, J. Am. Chem. Soc. **104**, 3295 (1982).
[8]Y. Kashimori, T. Kikuchi, and K. Nishimoto, J. Chem. Phys. **77**, 1904 (1982).
[9]A. V. Zolotariuk, K. H. Spatschek and E. W. Laedke, Phys. Lett. **101A**, 517 (1984).
[10]E. W. Laedke, K. H. Spatschek, M. Wilkens, and A. V. Zolotariuk, Phys. Rev. A **32**, 1161 (1985).
[11]M. Peyrad, St. Pnevmatikos, and N. Flytzanis, Phys. Rev. A **36**, 903 (1987).
[12]St. Pnevmatikos, Phys. Lett. **112A**, 249 (1987).
[13]R. Janoschek, in *The Hydrogen Bond*, edited by P. Schuster, G. Zundel, and C. Sandorfy (North-Holland, Amsterdam, 1976), Vol. 1, p. 165; J.-O. Lundgren and I. Olovson, *ibid.*, Vol. 2, p. 471.
[14]R. E. Rundle, J. Phys. **25**, 487 (1964).
[15]T. Schneider and E. Stoll, Phys. Rev. B **13**, 1216 (1976).
[16]L. V. Woodcock, Chem. Phys. Lett. **10**, 257 (1971).
[17]L. E. Reichl, *A Modern Course in Statistical Physics* (Arnold, London, 1980).